

# Origin of the chaotic motion of the Saturnian satellite Atlas

S. Renner<sup>1,2</sup>, N.J. Cooper<sup>3</sup>, M. El Moutamid<sup>4</sup>, B. Sicardy<sup>5</sup>, A. Vienne<sup>1,2</sup>, C.D. Murray<sup>3</sup>, M. Saillenfest<sup>2,6</sup>

Received \_\_\_\_\_; accepted \_\_\_\_\_

---

<sup>1</sup>Université Lille 1, Laboratoire d’Astronomie de Lille (LAL), 1 impasse de l’Observatoire, 59000 Lille, France

<sup>2</sup>Institut de Mécanique Céleste et de Calcul des Ephémérides (IMCCE), Observatoire de Paris, CNRS UMR 8028, 77 avenue Denfert-Rochereau, 75014 Paris, France

<sup>3</sup>Astronomy Unit, School of Physics and Astronomy, Queen Mary University of London, Mile End Road, London, E1 4NS, UK

<sup>4</sup>Department of Astronomy, Cornell University, Ithaca, NY 14853, USA

<sup>5</sup>LESIA/Observatoire de Paris, PSL, CNRS UMR 8109, University Pierre et Marie Curie, University Paris-Diderot, 5 place Jules Janssen, 92195 Meudon Cédex, France

<sup>6</sup>Department of Mathematics, University of Pisa, Italy

## ABSTRACT

We revisit the dynamics of Atlas. Using *Cassini* ISS astrometric observations spanning February 2004 to August 2013, Cooper et al. (2015) found evidence that Atlas is currently perturbed by both a 54:53 corotation eccentricity resonance (CER) and a 54:53 Lindblad eccentricity resonance (LER) with Prometheus. They demonstrated that the orbit of Atlas is chaotic, with a Lyapunov time of order 10 years, as a direct consequence of the coupled resonant interaction (CER/LER) with Prometheus. Here we investigate the interactions between the two resonances using the CoraLin analytical model (El Moutamid et al. 2014), showing that the chaotic zone fills almost all the corotation sites occupied by the satellite’s orbit. Four 70:67 apse-type mean motion resonances with Pandora are also overlapping, but these resonances have a much weaker effect. Frequency analysis allows us to highlight the coupling between the 54:53 resonances, and confirms that a simplified system including the perturbations due to Prometheus and Saturn’s oblateness only captures the essential features of the dynamics.

*Subject headings:* celestial mechanics – planets and satellites: dynamical evolution and stability – planets and satellites: individual (Atlas) – methods: analytical methods: numerical

## 1. Introduction

Thanks to the success of observing campaigns such as those using the Imaging Science Subsystem (ISS) of the *Cassini* orbiter, the short-term dynamical evolution of the small inner Saturnian satellites can now be studied with a high accuracy. This is important in order to give constraints on the physical origin and orbital evolution of these moons.

This work focuses on Atlas, the closest satellite to the outer edge of Saturn’s A ring. This satellite lies in a complex dynamical environment involving various mean motion resonances :

- 54 : 53 resonances between Atlas and Prometheus (Spitale et al. 2006; Cooper et al. 2015)
- 70 : 67 resonances between Atlas and Pandora (Spitale et al. 2006)
- 121 : 118 resonances between Prometheus and Pandora, leading to chaotic interactions every 6.2 years at closest approach (apse anti-alignment) (Goldreich & Rappaport 2003a,b; Renner & Sicardy 2003; Cooper & Murray 2004; Renner et al. 2005)
- 1 : 1 co-orbital resonance between Janus and Epimetheus
- 17 : 15 or 21 : 19 resonances between Prometheus or Pandora and Epimetheus (Cooper & Murray 2004)
- 3 : 2 near-resonances between Pandora and Mimas (French et al. 2003)

In fact, we show in this paper that Atlas is mainly perturbed by the 54 : 53 resonant perturbations from Prometheus. The latter involve two resonance arguments :

$\Psi_C = 54\lambda_{PR} - 53\lambda_{AT} - \varpi_{PR}$  and  $\Psi_L = 54\lambda_{PR} - 53\lambda_{AT} - \varpi_{AT}$ , corresponding to the Corotation Eccentricity Resonance (hereafter, CER) and the Lindblad Eccentricity Resonance (LER),

respectively (see El Moutamid et al. (2014) for a discussion). Here,  $\lambda$  represents the geometric mean longitude, while  $\varpi$  is the geometric longitude of pericentre. A ring of diffuse material discovered in *Cassini* images (Porco et al. 2004, 2005), R/2004 S1, shares Atlas’ orbit.

Spitale et al. (2006) fitted Voyager, HST and *Cassini* ISS observations of Atlas spanning the period 2004 May to 2005 October. They found periodic perturbations in Atlas’ orbit, with an amplitude of about 600 km along the orbital motion and a period of about 3 years, which they attributed to the 54:53 CER with Prometheus. They also identified the 70:67 mean motion resonance with Pandora (with an amplitude  $\sim 150$  km) and argued that since Prometheus and Pandora are interacting chaotically with each other, the orbit of Atlas itself might also be chaotic. More recently, Cooper et al. (2015) extended the timespan of *Cassini* ISS observations (2004-2013) to fit the orbits and the masses of the inner satellites. This timespan extension allowed to cover the most recent chaotic interaction between Prometheus and Pandora in February 2013, and the latest switch in the orbits of the co-orbitals Janus and Epimetheus in January 2010. They showed that Atlas is currently librating in both the 54:53 CER and the LER with Prometheus, making it yet another example of coupled CER/LER in the Saturn system, in common with Aegaeon, Anthe and Methone (El Moutamid et al. 2014; Spitale et al. 2006; Cooper et al. 2008; Hedman et al. 2009), and possibly the Neptune’s ring arcs (Namouni & Porco 2002; Renner et al. 2014). Using full numerical integrations combined with the FLI (Fast Lyapunov Indicator) time evolution, Cooper et al. (2015) showed that the orbit of Atlas is chaotic, with a short Lyapunov time of about 10 years.

In this paper, we confirm that the origin of chaos for Atlas is the coupled resonant interaction (CER/LER) with Prometheus. The interactions between the two resonances is investigated using the CoraLin analytical model (El Moutamid et al. 2014), showing that

the chaotic zone fills almost all the corotation sites occupied by the satellite’s orbit. We show that the four 70:67 overlapping apse-type mean motion resonances (see Table 3) due to Pandora have a much weaker effect on Atlas. We compare the results of the frequency analysis for the full numerical model fitted to *Cassini* observations (Cooper et al. 2015) and for a simplified system consisting of Saturn, Atlas and Prometheus only. The frequency analysis also allows us to study the effect of the coupling between the two 54:53 resonances on the existence and relevance of proper frequencies.

The paper is organized as follows. In Section 2, we provide an overview of the most recent ephemerides and resonant perturbations of Atlas. Section 3 summarizes the analytical modelling based the CoraLin model. This model is then numerically integrated in Section 4, using the orbital parameters of Atlas. Section 5 focuses on the frequency analysis, and a summary and discussion are given in Section 6.

## 2. Resonant perturbations from the most recent ephemerides

Cooper et al. (2015) fitted a numerical model to new *Cassini* ISS astrometric data for Atlas, Prometheus, Pandora, Janus and Epimetheus. The state vectors and masses were solved at the epoch 2007 JUN 01 00:00:00.0, and ephemerides spanning the period 2000 to 2020 were generated. Using the parameters of Saturn given in Table 1, the fitted state vectors are converted into geometric elements using the method of Renner & Sicardy (2006), and the solutions are summarized in Table 2. In Figure 1, we reproduce the longitude offsets of Atlas, Prometheus and Pandora relative to a linear ephemeris using mean motion values of 598.31312, 587.28501 and 572.78861 deg.day<sup>-1</sup>, respectively. Sudden and anti-correlated changes in mean motion appear for Prometheus and Pandora. These jumps result from chaotic interactions between the two moons due to the overlap of four 121:118 apse-type mean motion resonances (Goldreich & Rappaport 2003a; Renner & Sicardy

2003). As concluded by Farmer & Goldreich (2006), the changes in mean motion do not always correlate with pericentre anti-alignments. The  $\sim 1.7$  year oscillations of Pandora’s mean longitude are due to the nearby 3:2 CER with Mimas. Pandora’s semi-major axis lies approximately 50 km inside this resonance, and also 180 km inside the 3:2 LER with Mimas (French et al. 2003). Changes in mean motion are also apparent for Atlas, and the mean longitude is dominated by a  $\sim 4$  year oscillation, as a result of the 54:53 CER with Prometheus.

Cooper et al. (2015) showed numerically that the orbit of Atlas is chaotic with a Lyapunov time of order 10 years. On the other hand, since Prometheus and Pandora interact chaotically through 121:118 resonances, and since Atlas is perturbed by the 54:53 CER/LER with Prometheus, then the mean motion ratio of Atlas and Pandora is  $n_{AT}/n_{PA} = 1.044552$  (see Table 2), which is close to the 70 : 67 resonance. The figures 2 and 3 show the time variations of the resonance critical angles. Figure 2 displays the CER/LER arguments  $\Psi_C$  and  $\Psi_L$  on a timespan of 100 years. Between 2000 and 2020 both arguments are librating, except short episodes of circulation. These episodes occur around 2006 (resp. 2013) for the LER (resp. CER), while simultaneously the CER (resp. LER) argument is librating. The four 70:67 apse-type resonance arguments due to Pandora are displayed in Figure 3 between 2000 and 2020. These critical angles are :  $\Psi_1 = 70\lambda_{PA} - 67\lambda_{AT} - 3\varpi_{PA}$ ,  $\Psi_2 = 70\lambda_{PA} - 67\lambda_{AT} - 2\varpi_{PA} - \varpi_{AT}$ ,  $\Psi_3 = 70\lambda_{PA} - 67\lambda_{AT} - \varpi_{PA} - 2\varpi_{AT}$  and  $\Psi_4 = 70\lambda_{PA} - 67\lambda_{AT} - 3\varpi_{AT}$ . The four resonances overlap, but the separatrix crossings (where the critical angles go from a circulation motion to libration, or from libration to circulation) are not clearly correlated with the times of pericentre anti-alignments between Prometheus and Pandora (vertical black dashed lines), or Atlas and Pandora (dotted). Furthermore, the effect of this third-order resonance with Pandora on the dynamics of Atlas is much weaker than the CER/LER with Prometheus, as shown in Table 3 which lists the resonance libration rates and the perturbing function coefficients. From Figure 3, we note

that the angle  $\Psi_3$  is much closer to libration, on the timespan considered, than the three other critical arguments of the 70:67 resonance with Pandora. The next section details the analytical modelling of the motion of Atlas perturbed by Prometheus, in the framework of the elliptic planar restricted three-body problem.

### 3. Analytical Modelling

The mass ratio of Atlas and Prometheus is 0.036 (Cooper et al. 2015), and orbital inclinations for these two satellites are very small (Table 2). Therefore the motion of Atlas can be well-approximated using the CoraLin model (El Moutamid et al. 2014), which describes the behavior of a test particle near a horizontal first order mean motion resonance  $m + 1 : m$  with a perturbing satellite ( $m$  integer, here  $m = 53$ ), in the frame of the elliptic, planar, restricted three-body problem. According to this model, the motion of Atlas is described by a two degree of freedom system involving the two resonance critical angles  $\Psi_C$  and  $\Psi_L$ , after averaging the equations of motion over the rapidly varying angles. Then the coupled effects of the two resonant terms (CER/LER) can be studied through the following Hamiltonian :

$$\mathcal{H} = \frac{1}{2}(J_C - J_L)^2 - DJ_L - \varepsilon_C \cos(\Psi_C) - \varepsilon_L h, \quad (1)$$

with the equations of motion<sup>1</sup> :

---

<sup>1</sup>Note that the time scale used in the model is  $\tau = n_C t$ , where  $t$  is the usual time. Therefore, an object at CER has an orbital period  $T = 2\pi$ , and the dots in the equations are the derivatives with respect to  $\tau$ .

$$\begin{cases} \dot{J}_C = -\partial\mathcal{H}/\partial\Psi_C = -\varepsilon_C \sin(\Psi_C) \\ \dot{\Psi}_C = +\partial\mathcal{H}/\partial J_C = J_C - J_L \equiv \chi \\ \dot{h} = +\partial\mathcal{H}/\partial k = -(J_C - J_L + D)k \\ \dot{k} = -\partial\mathcal{H}/\partial h = +(J_C - J_L + D)h + \varepsilon_L. \end{cases} \quad (2)$$

The various quantities entering in (1) and (2) are defined in Table (4). The elements  $a$ ,  $e$  and  $\dot{\varpi}$  denote the geometric semi-major axis, eccentricity and orbital precession rate (forced by the planet’s oblateness), with subscripts  $S$  for the perturbing satellite (here Prometheus),  $a_C$  is the CER semi-major axis,  $n_C$  is the corresponding mean motion,  $\chi = \frac{3}{2}m\frac{a - a_C}{a}$  measures the Atlas’ distance from the exact CER, and  $M_S$  (resp.  $M$ ) is the mass of the satellite (resp. the central body). The terms  $A^m$  and  $E^m$  (cf. Table 3) are combinations of Laplace coefficients (Shu 1984). Here, these coefficients can be approximated by  $A^m \sim -E^m \sim 0.8m$  since  $|m|$  is large ( $m=53$ ). The first two equations of the system (2) describe the CER and the last two ones the LER. The coupling between the two resonances arise from (i) the  $J_L$  term in the second equation, which states how the particle orbital eccentricity driven by the LER perturbs the corotation pendulum motion, and (ii) the  $J_C$  term in the third and fourth equations, which indicates how the CER affects the motion of the eccentricity vector ( $h$ ,  $k$ ) associated with the LER. The CoraLin model has three fundamental parameters  $D$ ,  $\varepsilon_C$ ,  $\varepsilon_L$  :  $D$  is the (normalized) distance in frequency between the CER and the LER, indicative of the coupling,  $\varepsilon_C$  is the CER strength ( $n\sqrt{|\varepsilon_C|}$  the CER frequency), and  $\varepsilon_L$  represents the LER eccentricity forcing.

For  $D = 0$ , the CER and the LER are superimposed. Then the two degrees of freedom system (2) described by the Hamiltonian (1) admits a second integral of motion, and is thus integrable. This second integral was found by Sessin & Ferraz-Mello (1984) for the general case of two non-zero masses, and extended to the restricted case by Wisdom (1986), while being further analyzed by Henrard & Lemaître (1986). This result is rediscussed in



El Moutamid et al. (2014). As  $|D|$  increases, the coupling between the two resonances leads to chaotic motions as long as the LER radial location remains inside the CER site, see Figure 5 of El Moutamid et al. (2014) and the next Section.

For  $|D|$  large, the resonances are decoupled and can be treated separately, see El Moutamid et al. (2014). Actually, neglecting the LER for  $D$  large, the first two equations of the system (2) reduce to:

$$\begin{cases} \dot{\chi} = -\varepsilon_C \sin(\Psi_C) \\ \dot{\Psi}_C = \chi. \end{cases} \quad (3)$$

This simple pendulum model describes, in other contexts, the libration of a satellite in a spin-orbit resonance (Goldreich & Peale 1966), or the Neptune’s ring arcs confinement by the moon Galatea through a 42:43 resonance (Goldreich et al. 1986; Namouni & Porco 2002). Stable oscillations of  $\Psi_C$  occur around  $\Psi_C = 0$  (resp.  $\Psi_C = \pi$ ) for  $\varepsilon_C$  positive (resp. negative) with periods  $2\pi/n_C$ . The half-width of the CER site is given by  $\frac{4}{3}a_C \frac{\sqrt{\varepsilon_C}}{|m|}$ . Conversely, considering a perturbing satellite on a circular orbit,  $\varepsilon_C = 0$  and the CER vanishes. In this case  $J_C$  is the Jacobi constant, and the system (2) reduces to the classical second fundamental model for Lindblad resonance (Henrard & Lemaître 1983):

$$\begin{cases} \dot{h} = -(J_C - J_L + D)k \\ \dot{k} = +(J_C - J_L + D)h + \varepsilon_L. \end{cases} \quad (4)$$

The CoraLin model can be easily modified to implement satellite orbital migrations and explore scenarios of capture into CERs. The analytical estimate of capture probabilities is not an easy task, in particular when the eccentricity of the perturbing satellite is large enough so that the CER libration sites encompass the LER radius. El Moutamid et al. (2014) discussed the case of the small Saturnian satellites Anthe, Methone and Aegaeon, captured into CERs with Mimas (10 : 11, 14 : 15 and 7 : 6, respectively).

#### 4. Numerical integrations

Here we present representative results of numerical integrations of the CoraLin model, in the case of Atlas perturbed by the 54 : 53 CER/LER with Prometheus.

Figure 4 shows a comparison of the orbital elements (semi-major axis and eccentricity) as a function of time for Atlas, derived both from CoraLin (in red) and from a three-body simulation (black) including Atlas, Prometheus and Saturn’s oblateness (up to  $J_6$  included). The latter is actually presented in Figure 13 of Cooper et al. (2015). The initial conditions are given in Table 5, and are obtained from the ephemeris at epoch 2000 JAN 01 12:00:00.0 UTC (JED 2451545.0) by converting state vectors to geometric elements using the algorithm of Renner & Sicardy (2006). The integration of the averaged equations of motion of the Coralin model is in very good agreement with the full numerical model, confirming that the interactions of Atlas with Prometheus arising from the 54 : 53 resonances grabs the essential parts of the dynamics.

Surfaces of section  $(\Psi_C, \chi)$ , showing the topology of the CoraLin system described by (2), are presented in Figure 5. In these sections, the positions of Atlas (in red) with respect to the CER radial location are plotted every time the  $k$  component of the eccentricity vector is equal to zero. The reference radius  $\chi = 0$  corresponds to the CER radial location, and the LER radius at  $\chi = -D$  is indicated in blue. The surfaces of section start respectively on JED=2452647.6710 (2003 JAN 8, 04:06:14 UT), 2454303.0976 (2007 JUL 21, 14:20:32 UT), 2456142.4397 (2012 AUG 2, 22:33:10 UT) and 2458227.2788 (2018 APR 18, 18:41:28 UT), with initial orbital elements for Atlas and Prometheus derived from the three-body simulation shown in Figure 4. The values for Atlas’ elements are given in Table 6. To derive the location of the 54:53 CER ( $a_C = 137665.519$  km), we used the values for the mean motions and pericentre precession rates given in Table 2, and computed iteratively the semi-major axis which cancels the derivative of the resonance argument. The satellite

initial conditions, the CER radius  $a_C$  and the mass ratio between Prometheus and Saturn (from Table 1 and 2) are used to compute the values of the CoraLin parameters  $D$ ,  $\varepsilon_C$ ,  $\varepsilon_L$  given in Table 7. These parameters correspond to a CER half-width of 1.65 km (equivalent to  $\Delta\chi = 1$ ), a distance between the CER and the LER locations  $\frac{2}{3|m|}a_CD \sim -0.36$  km, and a libration period  $P_{\text{lib}} = 2\pi/(n\sqrt{|\varepsilon_C|}) = 3.45$  years. We note that the four satellites Anthe, Methone, Aegaeon and Atlas have very similar  $\varepsilon_L$  values, see Table 2 of El Moutamid et al. (2014).

The semi-major axis variations (Figure 4) places Atlas in different parts of the CoraLin phase space. The surfaces of section (Figure 5) show that Atlas alternates the chaotic or regular motions, with semi-major axis variations of amplitude  $\sim 1.5$  km comparable to the CER half-width. This is a different CoraLin regime compared to the cases of Aegaeon, Methone, Anthe which are embedded in arcs of material and have regular CoraLin orbits (El Moutamid et al. 2014). From the twenty years simulation (Figure 4), we estimate that episodes of chaotic motion (more precisely, orbital elements that correspond to chaotic orbits in the CoraLin phase space) add up to about 14 years. Note that we obtain the same phase portraits if we use initial conditions for Atlas and Prometheus derived from the ephemerides (Cooper et al. 2015), i.e. from integrations including the perturbations from all the other Saturnian satellites.

## 5. Frequency analysis

A conservative dynamical system can be described by its frequencies (Laskar et al. 1992). The frequency analysis is a method for studying the stability of orbits, based on a refined numerical search for a quasi-periodic approximation of its solutions over a finite time interval (Laskar 1990; Laskar et al. 1992; Laskar 1993). For regular motions, this technique has the advantage of giving rise to an analytical representation of the solutions.

It is also powerful for analysing weakly chaotic motion in hamiltonian systems. In this case, the frequencies obtained are not well defined and thus vary in time, with a rate related to the chaos strength. On the other hand, determining the frequencies that have influence on the orbital elements of the Saturnian moons (and how those frequencies eventually change with time) is important, as this can be helpful to study in detail the moon interactions, the resonances and their effects on the ring structures. In this aim we used the frequency analysis method, as described in e.g. Lainey et al. (2006).

Despite the chaotic motion of Atlas, we can obtain relevant results on the frequencies of the system by selecting suitable time intervals. We compare here the results of the frequency analysis of the full numerical model fitted to *Cassini* observations (Cooper et al. 2015) and a simplified system consisting of Saturn, Atlas, Prometheus only. This allows us to confirm the results obtained both with the CoraLin model (Section 4) or with the FLI simulations (Cooper et al. 2015).

We have examined the following systems :

- (1) the full numerical model fitted to *Cassini* observations (Figure 1)
- (2) a 3-body simplified system with the same initial conditions but consisting of Saturn, Atlas, Prometheus only
- (3) the same system as (2) but with an eccentricity for Prometheus  $e_{PR} = 2.8 \times 10^{-5}$
- (4) the same system as (2) but with Prometheus' orbit circular.

The dynamics of Atlas, perturbed by Prometheus, has the following characteristic timescales : (i) short periods ( $\sim 14$  hours) associated with the orbital frequency, (ii) precession periods ( $\sim 4$  months) associated with the apsidal precession rates  $\dot{\varpi}$ , (iii) libration periods ( $\sim 4$  and  $\sim 6$  years, respectively) associated with the CER and the LER,

and (iv) a Lyapunov time of the same order ( $\sim 10$  years).

In case (4) (Prometheus’ orbit circular), the CER is suppressed and in (3), the LER and the CER decouple since the Prometheus eccentricity value implies a half-width for the CER site of 0.18 km, i.e. half the distance between the LER and the CER. Therefore, the motion of Atlas is regular in these two examples, with the main perturbation arising from the LER, and the frequency analysis is very efficient. For example, Table 8 gives the solution for the semi-major axis of Atlas in the case (4). Given the timescales of the problem, the frequency analysis is performed on a time interval of 30 years, with a stepsize of 0.1 day. The series arguments are easily identified using the three fundamental frequencies of motion (mean motions for Atlas and Prometheus  $n_{AT}$  and  $n_{PR}$ , and LER libration frequency  $\nu_L$ ). Thus, the series is quasi-periodic, meaning that the case (4) corresponds to a regular motion. Comparable solutions are achieved for the other orbital elements of Atlas. For the case (3), where Atlas is trapped into the 54:53 LER and is close to but outside the CER, the analysis is less obvious because of the small eccentricity of Prometheus. Nevertheless, we are able to clearly identify the four fundamental frequencies of the (two degrees-of-freedom) system : the three previous ones,  $n_{AT}$ ,  $n_{PR}$ ,  $\nu_L$ , and the Prometheus’ pericentre precession rate  $\dot{\varpi}_{PR}$ . Furthermore, no significant variations of the frequencies (lower than  $10^{-5}$  deg.day $^{-1}$  for  $n_{AT}$  or  $10^{-3}$  deg.day $^{-1}$  for  $\nu_L$ ) are found by shifting the time interval chosen for analysis (30 years) on a 200 year numerical integration. This confirms that the case (3) corresponds to a regular motion too.

As expected, the method fails for the more realistic cases (1) or (2), as the system is chaotic on short time scales, with a Lyapunov time comparable to the resonance libration periods. The frequencies  $\dot{\Psi}_C$  and  $\dot{\Psi}_L$  are separated by a small distance  $\dot{\varpi}_S - \dot{\varpi} \simeq -0.124$  deg.day $^{-1}$ , whereas the CER half-width corresponds to a frequency difference of  $\sim 0.57$  deg.day $^{-1}$ . This overlap leads to chaotic motion. Chaos is visible, for instance, in the random

transitions of  $\Psi_C$  from libration to circulation (or from circulation to libration). Such transitions lead to opposite separatrix crossings of  $\Psi_L$ , which block out the determination of the frequencies on a given time interval. This is illustrated in Figure 2 for the model fitted to *Cassini* observations (case 1) and in Figure 6 for the 3-body system (case 2), both on a 100 year timespan. However, a partial representation of the frequencies for cases (1) and (2) can be obtained on time domains where no CER/LER separatrix crossings occur. The results are summarized in Table 9. The method is much less efficient than in the regular case because of chaos and reduced time intervals. Nevertheless, mean motion values and pericentre precession rates are well determined, allowing us to verify the resonance conditions. We notice that the time intervals considered are of the same order as the Lyapunov time, as expected. On the other hand, when the motion is sufficiently regular (i.e., no CER/LER transitions), the precision of the resonance rates (last column of Table 9) increases with the length of the time interval. The comparison of cases (1) and (2) shows that the essential part of Atlas’ dynamics is controlled by the interactions with Prometheus due to the 54:53 resonances.

We can identify the third-order resonant perturbations due to Pandora. Frequency analysis for the case (1) on the timespan 2006-2020 (where the 54:53 LER argument is librating, see Table 9) leads to  $\dot{\varpi}_{PA} = 2.599742 \text{ deg.day}^{-1}$  and a variation for  $\Psi_3 = 70\lambda_{PA} - 67\lambda_{AT} - \varpi_{PA} - 2\varpi_{AT}$  of  $0.0430 \text{ deg.day}^{-1}$ . This value is about ten times smaller than the variations of the three other 70:67 arguments, confirming that the angle  $\Psi_3$  seen in Figure 3 looks closer to libration. Furthermore, separatrix crossings for  $\Psi_3$  occur at the same epochs as those of the 54:53 LER argument  $54\lambda_{PR} - 53\lambda_{AT} - \varpi_{AT}$ . Further work is needed to explain if this is purely coincidental or not.

We have also verified that by increasing the eccentricity of Prometheus, e.g. by a factor of ten ( $e_{PR} = 2 \times 10^{-2}$ ), Atlas’ motion becomes extremely chaotic with a very short

Lyapunov time, and an impossibility to compute the main frequencies. This was already shown in El Moutamid et al. (2014) when the resonances are superimposed ( $D \ll 1$ ).

When the eccentricity of the perturbing satellite is small enough so that the two resonances are well separated, i.e. when the CER half-width is smaller than the distance of the LER from the CER ( $\varepsilon_C < D$ ), the motion becomes regular. Here, the limit case between regular and chaotic motions corresponds to a small eccentricity  $e_{PR} \sim 8 \times 10^{-5}$ .

## 6. Summary and Discussion

Using initial states and masses fitted to new *Cassini* ISS observations, Cooper et al. (2015) developed an improved high-precision numerical model for the orbits of Atlas, Prometheus, Pandora, Janus and Epimetheus. Based on this model, we confirmed that the orbit of Atlas is chaotic, as a consequence of the coupled interaction between the 54:53 CER and LER with Prometheus. We showed that the chaotic region fills almost all the CER site occupied by Atlas’ orbit, and highlighted the 70:67 overlapping resonances with Pandora. The frequency analysis allowed us to confirm our results, showing that the dynamics of Atlas is mostly controlled by the 54:53 resonant perturbations from Prometheus. A partial representation of the frequencies of motion was obtained on timespans comparable to the Lyapunov time of the system, where no separatrix crossings occur. We showed that Atlas motion is chaotic as soon as Prometheus’ eccentricity exceeds a value of about  $8 \times 10^{-5}$ . The smallness of this value suggests that the CER/LER coupling and the resulting chaotic motions could be a relatively common process during the orbital evolution of small, nearby moons around Saturn, as the satellite orbits expand through the transfer of angular momentum from the rings and cross numerous mean motion resonances. Similar chaotic interactions could be frequent as part of the orbital evolution of satellites around other giant planets, and require further investigation. Indeed, recent works showed that

the closely-packed Uranian system of inner low-mass satellites is configured in chains of interlinked first- and second-order eccentric resonances, contributing to chaotic motions (French et al. 2012; Quillen & French 2014; French et al. 2015). It also remains to assess the possible consequences of the dynamical results presented here on the orbital evolution timescales.

This work was supported by the Science and Technology Facilities Council (Grant No. ST/M001202/1) and Cooper and Murray are grateful to them for financial assistance. Murray is grateful to The Leverhulme Trust for the award of a Research Fellowship. Cooper thanks the University of Lille 1 for additional funding while he was an invited researcher at the Lille Observatory. Cooper, El Moutamid, Murray, Renner and Vienne thank the Encelade working group for interesting discussions.



## REFERENCES

- Cooper, N.J., Murray, C.D., 2004, AJ, 127, 1204-1217.
- Cooper, N.J., Murray, C.D., Beurle, K., Evans, M.W., Jacobson, R. A., Porco, C.C., 2008, Icarus, 195, 765-777.
- Cooper, N.J., Renner, S., Murray, C.D., Evans, M.W., 2015, AJ, 149, 27.
- El Moutamid, M., Sicardy, B., Renner, S., 2014, Celest. Mech. and Dyn. Astron., 118, 235-252.
- Farmer, A.J., Goldreich, P., 2006, Icarus, 180, 403-411.
- French, R.G., McGhee, C.A., Dones, L., Lissauer, J.J., 2003, Icarus, 162, 143-170.
- French, R.S., Showalter, M.R., 2012, Icarus, 220, 911.
- French, R.G., Dawson, R.I., Showalter, M.R., 2015, AJ, 149, 142.
- Goldreich, P., Peale, S., AJ, 1966, 71, 425.
- Goldreich, P., Tremaine, S., Ann. Rev. Astron. Astrophys., 1982, 20, 249-283.
- Goldreich, P., Tremaine, S., Borderies, N., 1986, AJ, 92, 490-494.
- Goldreich, P., Rappaport, N., 2003, Icarus, 162, 391-399.
- Goldreich, P., Rappaport, N., 2003, Icarus, 166, 320-327.
- Hedman, M.M., Cooper, N.J., Murray, C.D., Beurle, K., Evans, M.W., Tiscareno, M.S., Burns, J.A., 2009, Icarus, 207, 433-447.
- Henrard, J., Lemaitre, A., 1983, Celest. Mech. and Dyn. Astron., 30, 197-218.
- Henrard, J., Lemaitre, A., 1986, Celest. Mech. and Dyn. Astron., 39, 213-238.

- Jacobson, R. A., Spitale, J., Porco, C. C., Beurle, K., Cooper, N. J., Evans, M. W., Murray, C. D., 2008, *AJ*, 135, 261-263.
- Laskar J., 1990, *Icarus*, 88, 266-291.
- Laskar J., Froeschlé, C., Celletti, A., 1992, *Physica D*, 56, 253-269.
- Laskar J., 1993, *Physica D*, 67, 257.
- Lainey V., Duriez L. and Vienne A., 2006, *A&A*, 456, 783-788.
- Murray, C.D., and Dermott, S.F., 1999, *Solar System Dynamics*, Cambridge University Press, Cambridge, U.K.
- Namouni, F., Porco, C. C., 2002, *Nature*, 417, 45-47.
- Porco, C.C., et al., 2004, *IAU Circ.* 8401, 1.
- Porco, C.C., Baker, E., Barbara, J., et al., 2005, *Science*, 307, 1226-1236.
- Quillen, A.C., French, R.S., 2014, *MNRAS*, 445, 3959.
- Renner, S., Sicardy, B., 2003, *BAAS*, 35(4), Div. Dyn. Astron. abstr. No. 10.02.
- Renner, S., Sicardy, B., French, R.G., 2005, *Icarus*, 174, 230-240.
- Renner, S., Sicardy, B. 2006, *Celest. Mech. and Dyn. Astron.*, 94, 237-248.
- Renner, S., Sicardy, B., Souami, D., Carry, B., Dumas, C., 2014, *A&A*, 563, A133.
- Sessin, W., Ferraz-Mello, S., 1984, *Celest. Mech. and Dyn. Astron.*, 32, 307332.
- Spitale, J.N., Jacobson, R.J., Porco, C.P., Owen, W.M., 2006, *AJ*, 132, 692-710.
- Shu, F.H., 1984, *IAU Colloq. 75: Planetary Rings*, Greenberg, R. and Brahic, A. Eds, 513-561.

Wisdom, J., 1986, *Celest. Mech. and Dyn. Astron.*, 38, 175180.

Table 1. Saturn constants, from Cooper et al. (2015).

Constant	Value	units
$GM$	$3.793120706585872 \times 10^7$	$\text{km}^3 \text{ s}^{-2}$
Radius	60330	km
$J_2$	$1.629084747205768 \times 10^{-2}$	
$J_4$	$-9.336977208718450 \times 10^{-4}$	
$J_6$	$9.643662444877887 \times 10^{-5}$	

Table 2. Geometric orbital elements for Atlas, Prometheus and Pandora at epoch 2007 JUN 01 00:00:00.0 UTC (JED 2454252.50075446), computed from fits to *Cassini* observations (Cooper et al. 2015). The elements  $a$ ,  $e$ ,  $i$ ,  $\Omega$ ,  $\varpi$ ,  $\lambda$  are respectively the semi-major axis, the eccentricity, the inclination, the longitude of ascending node, the longitude of pericentre, and the mean longitude. The mean motion and the pericentre precession rate are computed self-consistently from the semi-major axis using the Saturn constants given in Table 1.

	Atlas	Prometheus	Pandora
Mass (kg)	$5.751 \times 10^{15}$	$1.600 \times 10^{17}$	$1.368 \times 10^{17}$
$a$ (km)	137664.946	139378.239	141711.251
$n$ (deg.day $^{-1}$ )	598.316026	587.283454	572.796769
$e$	0.00114	0.00222	0.00417
$i$ (deg)	0.00290	0.00753	0.05024
$\Omega$ (deg)	21.19790	86.59026	339.90039
$\varpi$ (deg)	325.55527	263.32452	52.27079
$\dot{\varpi}$ (deg.day $^{-1}$ )	2.881135	2.757159	2.599218
$\lambda$ (deg)	310.40476	50.69084	281.02045

Table 3. Resonance arguments, rates, periods, coefficients. The rates are the time derivatives  $\dot{\Psi}$  of the resonance angles, computed using the mean motion values and the pericentre precession rates given in Table 2, and the periods are  $2\pi/\dot{\Psi}$ . The corresponding terms of the disturbing potential are given in the last column. The coefficients  $f_i$  are combinations of Laplace coefficients (Shu 1984),  $A^m = -[f_{27} + e_{AT}^2 f_{28} + e_{PR}^2 f_{29}]$ ,  $E^m = -[f_{31} + e_{AT}^2 f_{32} + e_{PR}^2 f_{33}]$ , keeping the terms up to order 3 in eccentricities in the potential and evaluating the coefficients  $f_i$  at  $\alpha = a_{AT}/a_{PR}$  in the tables of Murray & Dermott (1999).

Argument	Rate (deg.day <sup>-1</sup> )	Period (yr)	Coefficient ( $\times 10^{-9}$ m <sup>2</sup> .s <sup>-2</sup> )
$\Psi_L = 54\lambda_{PR} - 53\lambda_{AT} - \varpi_{AT}$	-0.324494	3.03743	$(Gm_{PR}/a_{PR})e_{AT}A^m = 3.7976$
$\Psi_C = 54\lambda_{PR} - 53\lambda_{AT} - \varpi_{PR}$	-0.200518	4.91540	$(Gm_{PR}/a_{PR})e_{PR}E^m = -7.4585$
$\Psi_1 = 70\lambda_{PA} - 67\lambda_{AT} - 3\varpi_{PA}$	0.800002	1.23203	$(Gm_{PA}/a_{PA})e_{PA}^3 f_{85} = 0.0847$
$\Psi_2 = 70\lambda_{PA} - 67\lambda_{AT} - 2\varpi_{PA} - \varpi_{AT}$	0.518085	1.90244	$(Gm_{PA}/a_{PA})e_{PA}^2 e_{AT} f_{84} = -0.0680$
$\Psi_3 = 70\lambda_{PA} - 67\lambda_{AT} - \varpi_{PA} - 2\varpi_{AT}$	0.236169	4.17339	$(Gm_{PA}/a_{PA})e_{PA}e_{AT}^2 f_{83} = 0.0182$
$\Psi_4 = 70\lambda_{PA} - 67\lambda_{AT} - 3\varpi_{AT}$	-0.0457478	21.5448	$(Gm_{PA}/a_{PA})e_{AT}^3 f_{82} = -0.0016$



Table 4. Variables and parameters used in the CoraLin model (El Moutamid et al. 2014), see text Section 3 for details. The coefficients  $A^m$  et  $E^m$  are defined in the caption of Table

3.

Quantities	Definitions
$h$	$\sqrt{3} \mid m \mid e \cos(\Psi_L) = \sqrt{2J_L} \cos(\Psi_L)$
$k$	$\sqrt{3} \mid m \mid e \sin(\Psi_L) = \sqrt{2J_L} \sin(\Psi_L)$
$J_L$	$(h^2 + k^2)/2 = 3m^2 e^2/2$
$J_C$	$\chi + J_L = 3m(a - a_C)/(2a_C) + J_L$
$\varepsilon_L$	$\sqrt{3} \mid m \mid (M_S/M)(a_C/a_S)A^m$
$\varepsilon_C$	$3m^2(M_S/M)(a_C/a_S)E^m e_S$
$D$	$(\dot{\varpi}_S - \dot{\varpi})/n_C$

Table 5. Initial conditions for the simulations of Figure 4.

	Atlas	Prometheus
$a$ (km)	137666.519	139378.180
$e$	0.00117	0.00222
$\varpi$ (deg)	87.97515	357.21193
$\lambda$ (deg)	116.02563	203.51184



Table 6. Initial conditions for Atlas used for the surfaces of section of Figure 5.

Prometheus moves on an unperturbed orbit with elements given in Table 2.

	2003 JAN 8	2007 JUL 21	2012 AUG 2	2018 APR 18
$a$ (km)	137664.290	137665.545	137666.696	137664.800
$e$	0.00118	0.00105	0.00106	0.00109
$\varpi$ (deg)	259.75152	345.53665	243.35908	119.44170
$\lambda$ (deg)	111.26215	216.09571	199.10884	181.89609

Table 7. CoraLin parameters for Atlas. For comparison with Anthe, Methone and Aegaeon, the values are also provided in the nomenclature of El Moutamid et al. (2014),

where  $\varepsilon_C \equiv 1$ .

$\varepsilon_C$	$D$	$\varepsilon_L$
$-2.28 \times 10^{-7}$	$-2.07 \times 10^{-4}$	$1.11 \times 10^{-6}$
1	-0.43	0.11

Table 8. Frequency analysis for the semi-major axis of Atlas in the case (4) of Section 5 (Prometheus on a circular orbit). The time is from 2007 JUN 01 00:00:00.0 UTC. The time interval used is 30 years with a stepsize of 0.1 day. The three fundamental frequencies are used for the identification of the arguments of the series terms. These frequencies are the LER libration frequency  $\nu_L$ , the mean mean motion of Atlas  $n_{AT}$ , and the one of Prometheus  $n_{PR}$ . The frequency values derived from this run are respectively  $\nu_L = 0.153114 \text{ deg.day}^{-1}$ ,  $n_{AT} = 598.309930 \text{ deg.day}^{-1}$  and  $n_{PR} = 587.283438 \text{ deg.day}^{-1}$ .

The series is expressed in cosine.

Number	Amplitude (km)	Frequency (deg.day <sup>-1</sup> )	Phase (deg)	Identification
1	137665.87876	0	0	-
2	0.87952	0.153114	179.83	$\nu_L$
3	0.03816	0.459343	179.49	$3\nu_L$
4	0.01224	10.873434	-100.51	$n_{AT} - n_{PR} - \nu_L$
5	0.01188	11.179667	79.11	$n_{AT} - n_{PR} + \nu_L$
6	0.01094	0.306233	179.65	$2\nu_L$
7	0.01054	22.052890	160.11	$2n_{AT} - 2n_{PR}$
8	0.00946	33.079410	59.64	$3n_{AT} - 3n_{PR}$
9	0.00868	44.105919	-40.77	$4n_{AT} - 4n_{PR}$
10	0.00806	55.132426	-141.13	$5n_{AT} - 5n_{PR}$
...				



Table 9. Frequency analysis for the chaotic cases (1) and (2) of Section 5. The values are in  $\text{deg.day}^{-1}$ . The last column gives the rates  $54n_{PR} - 53n_{AT} - \dot{\varpi}_{AT}$  (LER) or  $54n_{PR} - 53n_{AT} - \dot{\varpi}_{PR}$  (CER), i.e. the difference with the exact resonance condition.

Time interval	$n_{AT}$	$n_{PR}$	$\dot{\varpi}_{AT}$	$\dot{\varpi}_{PR}$	LER/CER	Rate
Case (1)						
2000-2012	598.314000	587.284665	2.879580	2.757720	CER	-0.0278
1950-2010	598.311138	587.282364	2.881033	2.757703	CER	-0.0004
2006-2020	598.311003	587.285110	2.879606	2.757686	LER	0.0332
Case (2)						
2050-2080	598.312204	587.283466	2.879486	2.757168	CER	0.0031
2020-2080	598.312277	587.283466	2.879626	2.757168	CER	-0.0007
2000-2016	598.309703	587.283467	2.878903	2.757168	LER	0.0140
2087-2102	598.309497	587.283465	2.880308	2.757168	LER	0.0235

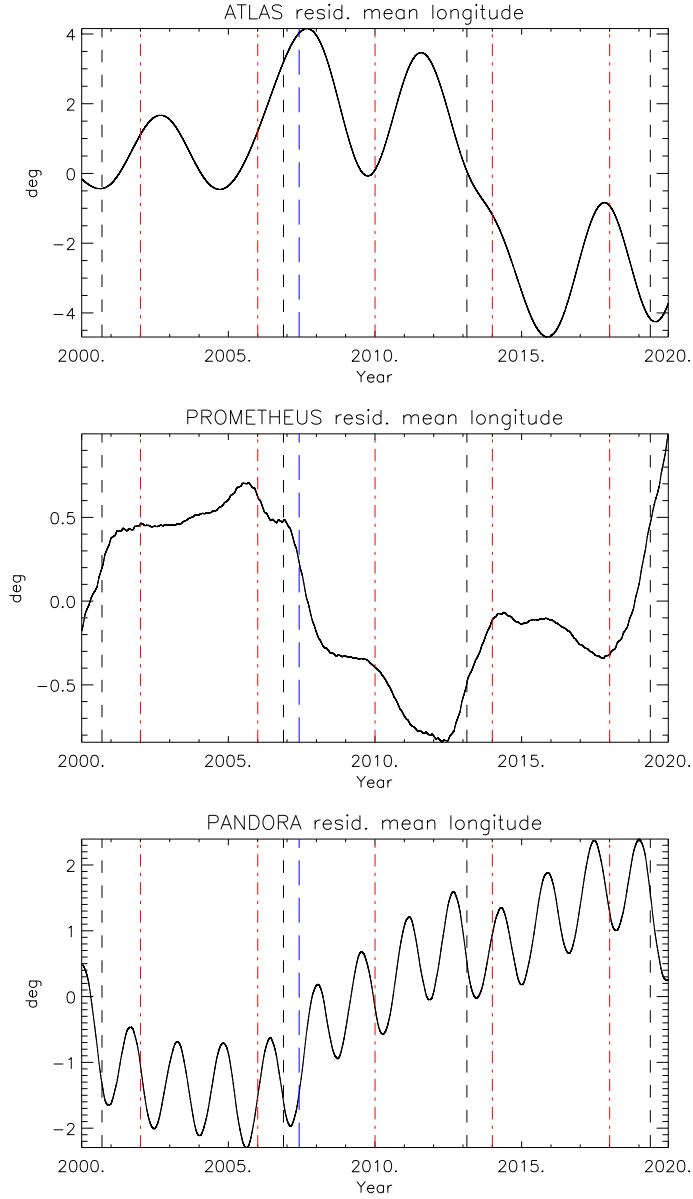


Fig. 1.— Residual Mean Longitudes for (a) Atlas, (b) Prometheus and (c) Pandora between 2000 and 2020 from the full numerical model of Cooper et al. (2015). *Cassini* astrometric observations spanning 2004 February to 2013 August have been used to fit the orbits and the satellite masses. Linear background trends have been subtracted from the mean longitudes using rates of (a) 598.31312 deg/day, (b) 587.28501 deg/day and (c) 572.78861 deg/day. Vertical black dashed lines mark times of closest approach between Prometheus and Pandora. Vertical red dot-dashed lines mark times of switches in the configuration of Janus and Epimetheus. Vertical blue line marks fit epoch. This figure is a reproduction of

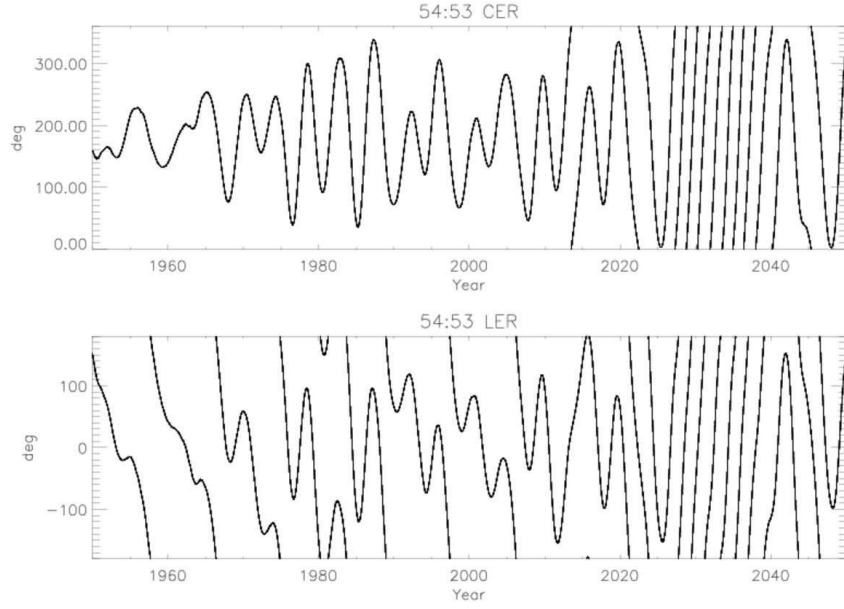


Fig. 2.— 54 : 53 CER and LER arguments for Atlas and Prometheus from the full numerical model of Cooper et al. (2015), extended to 100 years between 1950 and 2050. The angles are (a)  $\Psi_C = 54\lambda_{PR} - 53\lambda_{AT} - \varpi_{PR}$  and (b)  $\Psi_L = 54\lambda_{PR} - 53\lambda_{AT} - \varpi_{AT}$ . Random transitions of  $\Psi_C$  from libration to circulation (or from circulation to libration) occur, with opposite separatrix crossings of  $\Psi_L$ , e.g. around 2013 or 2022.

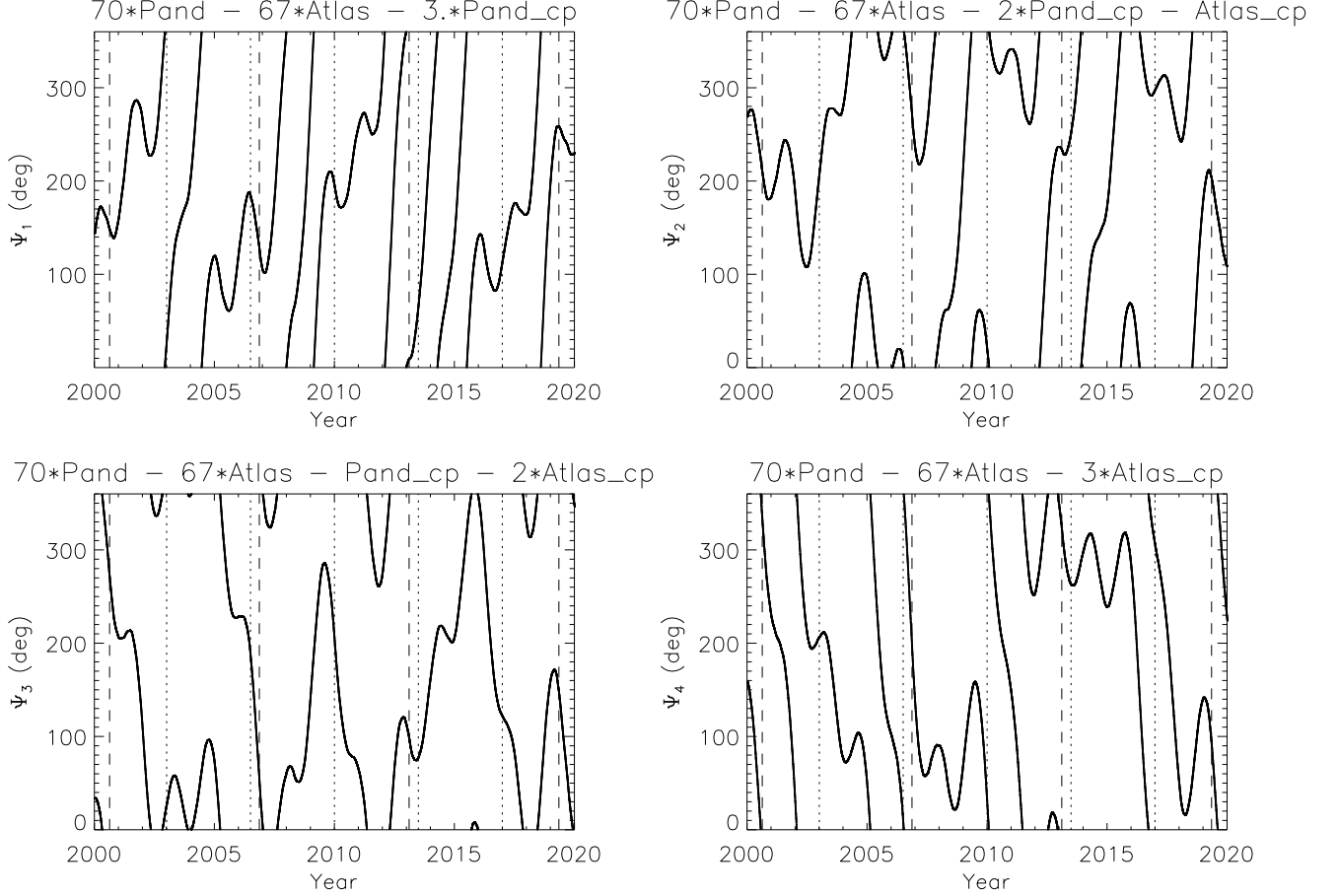


Fig. 3.— 70 : 67 resonance arguments for Atlas and Pandora between 2000 and 2020 from the full numerical model of Cooper et al. (2015). The angles are (a)  $\Psi_1 = 70\lambda_{PA} - 67\lambda_{AT} - 3\varpi_{PA}$ , (b)  $\Psi_2 = 70\lambda_{PA} - 67\lambda_{AT} - 2\varpi_{PA} - \varpi_{AT}$ , (c)  $\Psi_3 = 70\lambda_{PA} - 67\lambda_{AT} - \varpi_{PA} - 2\varpi_{AT}$  and (d)  $\Psi_4 = 70\lambda_{PA} - 67\lambda_{AT} - 3\varpi_{AT}$ . Vertical black dashed (resp. dotted) lines mark times of apse anti-alignments between Prometheus and Pandora (resp. Atlas and Pandora). The four resonances overlap, but the separatrix crossings are not clearly correlated with the times of pericentre anti-alignments. The angle  $\Psi_3$  is much closer to libration than the three other resonance arguments.

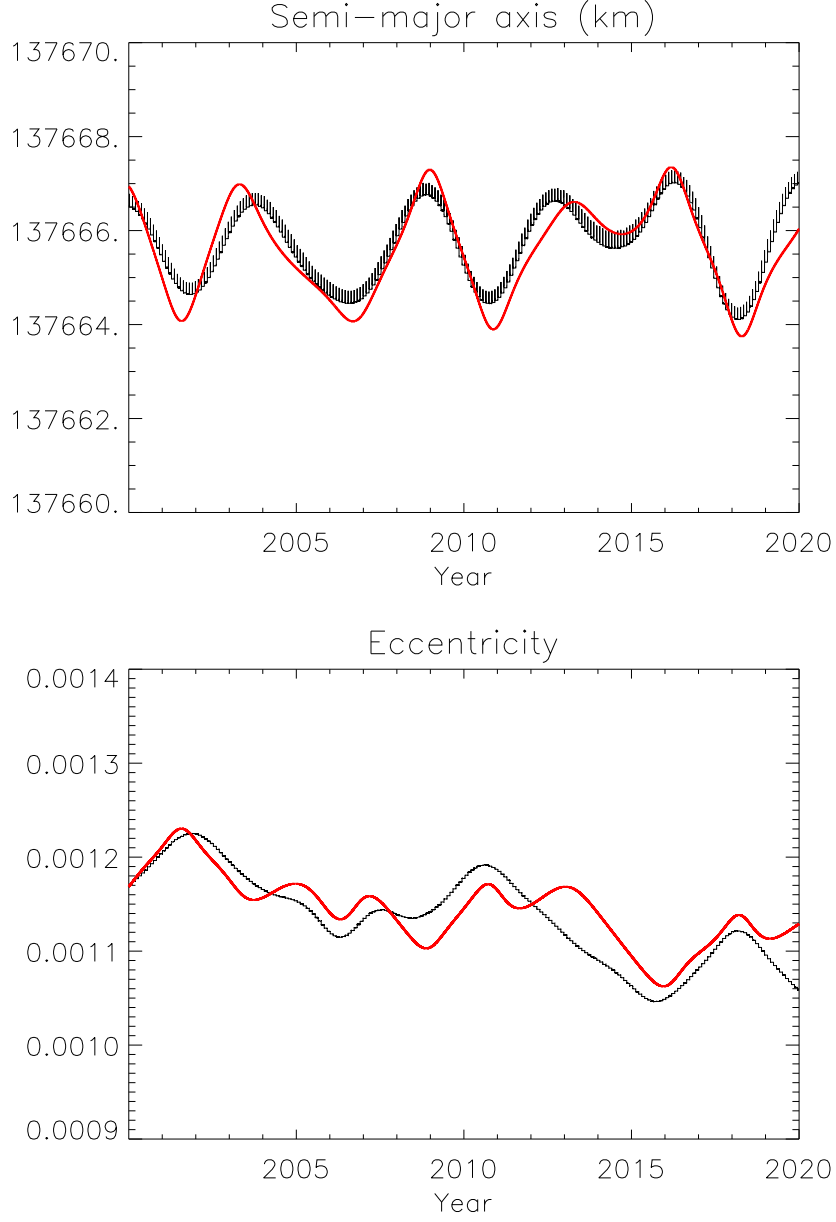


Fig. 4.— Semi-major axis and eccentricity for Atlas between 2000 and 2020. The red curve is given by the CoraLin model, and the black curve is from a full numerical integration including Prometheus and Saturn’s oblateness up to and including terms in  $J_6$ .



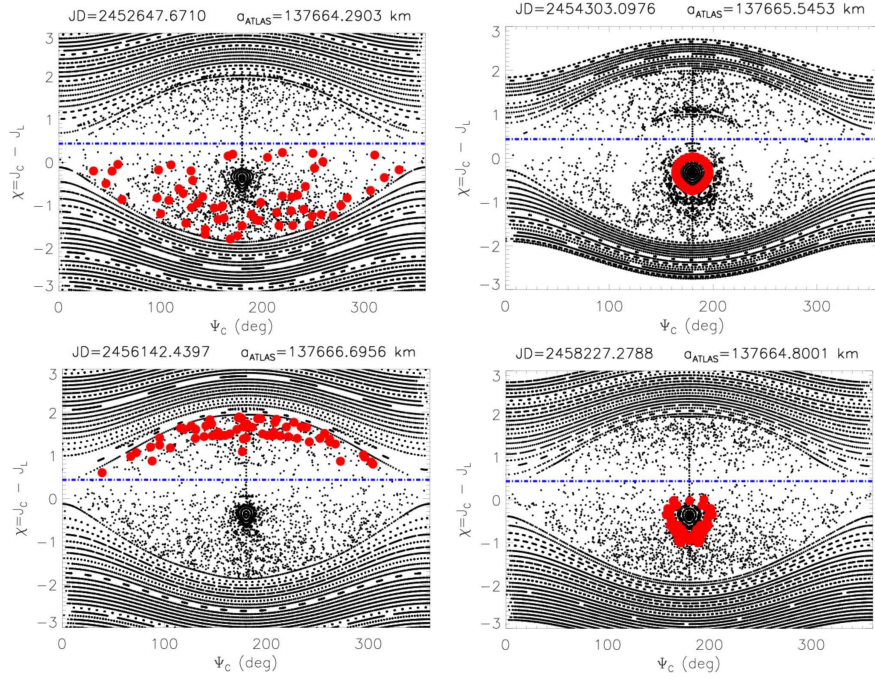


Fig. 5.— CoraLin surfaces of section  $(\Psi_C, \chi)$  starting on 2003 JAN 8, 2007 JUL 21, 2012 AUG 2, 2018 APR 18. The LER radius at  $\chi = -D$  is in blue. Atlas is in red, using initial conditions (see Table 6) from the three-body simulation Saturn, Prometheus, Atlas shown in Figure 4. For each surface, the integration time is 550 years.

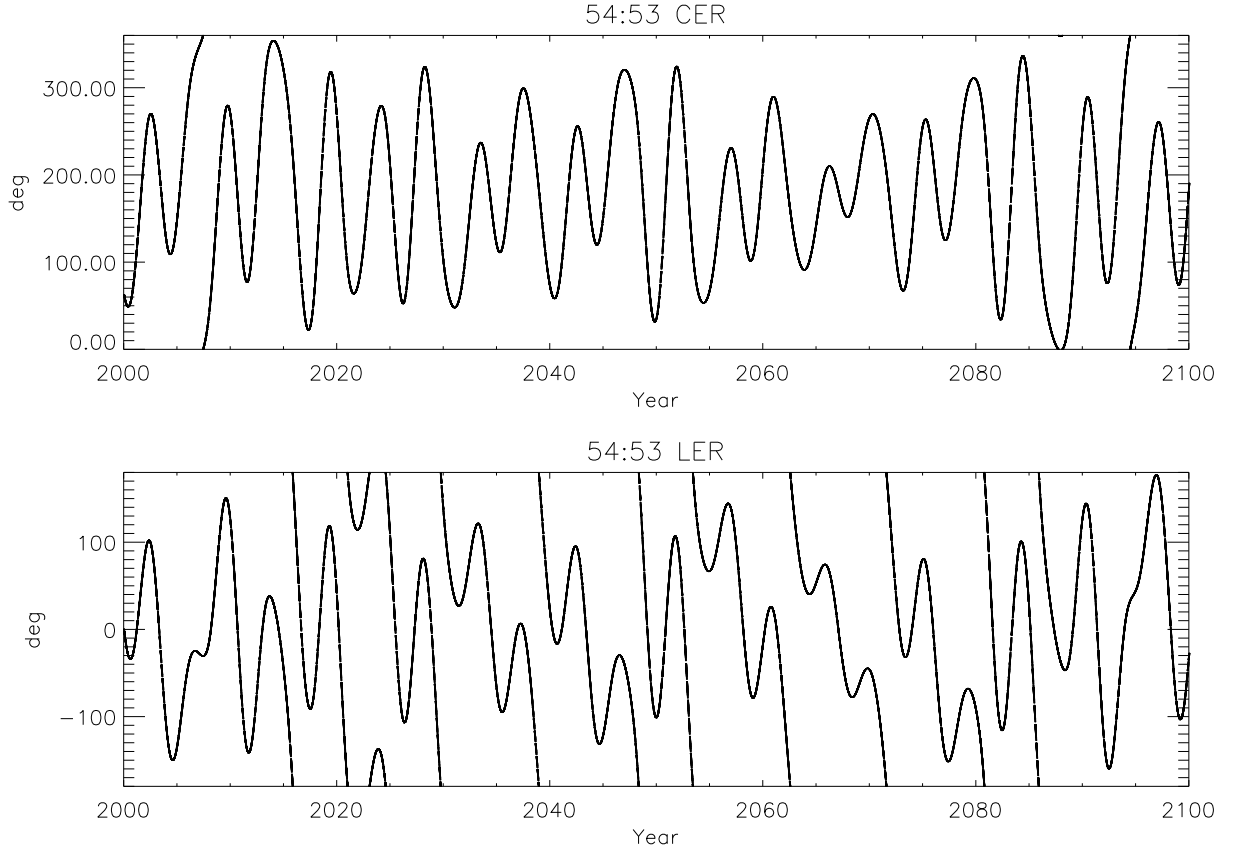


Fig. 6.— 54 : 53 CER and LER arguments for Atlas and Prometheus between 2000 and 2100 from a three-body model consisting of Atlas, Prometheus and Saturn (case 2 of Section 5). As in Figure 2, chaos is visible in the random CER/LER separatrix crossings, which prevent the determination of frequencies on arbitrary time intervals, see Table 9.